Effect of Recycled Concrete Aggregate Replacement Level on the Fracture Behavior of Concrete

Mahdi Arezoumandi[*1], Jonathan Drury[2], Jeffery S. Volz[3]

School of Civil Engineering and Environmental Science, University of Oklahoma, 423 Carson Engineering Center, 202 W. Boyd St., Norman, OK, USA

[*1]ma526@mst.edu; [2]jtdvg9@mst.edu; [3]volz@ou.edu

***Abstract*- This study presents the results of an experimental investigation that evaluates the effect of recycled concrete aggregate replacement level on the fracture energy of concrete. This study includes five mixes with 0, 30, 50, 70, and 100% recycled concrete aggregate as a coarse aggregate replacement. This experimental program consisted of 20 fracture beams to study the fracture behavior of concrete. The experimental fracture energies were compared with the fracture energy provisions of different design codes and also different analytical equations. Furthermore, statistical data analyses (both parametric and non-parametric) were performed to evaluate whether or not there is any statistically significant difference between the experimental fracture energies of different mixes. Results of these statistical tests show that the mix with higher level of recycled concrete aggregate replacement level has lower fracture energy.**

Keywords- Fracture Energy; Recycled Concrete Aggregate; Virgin Concrete Aggregate

I. INTRODUCTION

Recently, there has been an increasing trend toward the use of sustainable materials, which improves the environment by reducing the consumption of non-renewable natural resources. Concrete - the second most consumed material in the world after water– uses a significant amount of non-renewable resources. As a result, numerous researchers have investigated the use of recycled materials in the production of concrete such as fly ash [1-4] and recycled aggregate [5-7].

Unfortunately global data on concrete waste generation are unavailable, but construction and demolition waste accounts for around 900 million tons annually just in Europe, the US, and Japan [8]. Recycling concrete not only reduces the use of virgin aggregate but also decreases landfills.

Comprehensive research has been done on both the fresh and hardened properties of recycled concrete aggregate (RCA), but there are just a few studies on the fracture behavior of RCA. Since fracture energy plays a significant role in determining shear [9-11] and bond strength [12] of concrete structures, it is important to evaluate the effect of RCA replacement on the fracture energy of concrete.

Bordelon et al. [6] used 50% and 100% recycled concrete aggregate as a coarse aggregate replacement and reported a lower fracture energy for 100% recycled concrete aggregate and a similar fracture energy for 50% recycled concrete aggregate compared with the conventional concrete (CC). Casuccio et al. [7] used three different compressive strength levels concrete of RCA and reported 27 to 45% reduction on fracture energy compared with CC.

II. RESEARCH SIGNIFICANCE

It is found that few fracture energy tests of RCA were carried out in the present literature. . Without this background, there is no quantitative basis for safely implementing RCA in structural design. Consequently, the authors, in conjunction with the Missouri Department of Transportation (MoDOT), developed a testing plan to evaluate fracture energy of RCA specimens with local materials. The investigators developed RCA mixes that covered the range of potential mix designs used by MoDOT in the construction of transportation-related infrastructure. The experimental program, test results, and analyses for this study are presented in the following discussion.

III. EXPERIMENTAL PROGRAM

A. Materials and Mix Design

For the CC mix, ASTM Type I Portland cement and the crushed limestone with a maximum nominal aggregate size of 25 mm from Jefferson City Dolomite (Jefferson City, MO) were used. The fine aggregate was natural sand from Missouri River Sand (Jefferson City, MO).

This mix design was used to construct control specimens to serve as baseline comparisons to the RCA mix and will also serve as parent material for the RCA source. The resulted concrete was ground into aggregate with a maximum nominal aggregate size of 25 mm. Test results for the coarse aggregate used in the CC mix design as well as the results of the RCA are shown in Table 1. As expected, the RCA had lower specific gravity and unit weight and considerably higher absorption. The

Los Angeles abrasion test results were virtually identical. The RCA contained 46.1% residual mortar (by weight).

The concrete mixture proportions are given in Table 2. Concrete mixtures included a CC as a control mix and also RCA -30%, RCA -50%, RCA -70%, and RCA -100% as the mixes utilize a 30%, 50%, 70%, and100% RCA as a virgin aggregate replacement by volume, respectively.

TABLE 1 Aggregate Properties

Property	CC	RCA
Bulk Specific Gravity, Oven-Dry	2.72	2.35
Dry-Rodded Unit Weight, (kg/m^3)	1600	1440
Absorption (%)	0.98	4.56
LA Abrasion (% Loss)	43	41

TABLE 2 Mixture Proportions of Concrete

Mixture	Cement kg/m3	Fine aggregate kg/m3	Coarse aggregate kg/m3	Recycled Coarse aggregate kg/m3	AE kg/m3	HRWR liter	w/cm
CC	315	725	1150	-	0.62	1.65	0.45
RCA-30	315	725	810	300	0.62	1.65	0.45
RCA-50	315	725	580	500	0.62	1.65	0.47
RCA-70	315	725	350	700	0.62	1.65	0.47
RCA-100	315	800	-	1000	0.62	1.65	0.5

B. Fracture energy

Fracture energy is defined as the amount of energy necessary to create a crack of unit surface area projected in a plane parallel to the crack direction. Hillerborg [13] provided a theoretical basis for a concrete fracture energy testing procedure, often referred to as the work-of-fracture method (WFM), in which the fracture energy is computed as the area under the experimental load-deflection response curve – for a notched concrete beam subjected to three-point bending – is divided by the projected area of the fractured concrete. In other words, when conducting a three-point bending test on a notched beam, as the beam splits into two halves, the fracture energy (GF) can be determined by dividing the total dissipated energy by the projected surface area of the crack as shown in Equation 1.

$$G_F = \frac{W}{b\,(d-a_o)} \tag{1}$$

where W is the total energy dissipated in the test, and b, d, and ao are the thickness, height, and notch depth of the beam, respectively. The same approach was adopted by the RILEM standard [14].

For the current study, the researchers performed fracture energy tests using the three-point, notched specimen, bend test. The beam specimens were measured 150×150×600 mm with a span length of 450 mm. The notch – which was cast into the concrete as opposed to being saw cut after the concrete hardened – had a depth of 40 mm and a thickness of 6 mm. A clip gauge measured the crack mouth opening displacement (CMOD), two linear variable differential transducers (LVDTs) measured deflection at the mid-span of the beam, and self-weight compensation was provided through lever arms (Figure 1). The tests were performed using a closed loop, servo-controlled MTS machine at a loading rate of 0.002 mm/s.

A total of 20 specimens (four for each concrete type) were constructed for fracture energy tests. After casting, the beam specimens and companion compressive strength cylinders were moistly cured until they were tested for 28 days.

IV. Experimental Results and Discussion

The following section presents the results of the test program and discusses the effect of RCA replacement level on the fracture energy of concrete.

A. Fracture energy test results

Results of the fracture energy tests for all mixes are presented in Table 3 along with the corresponding compressive strengths at the time of testing. Also included in Table 4 are theoretical fracture energies based on relationships proposed by Bazant et al.[15], the JSCE-07 "Standard Specifications for Concrete Structures," [16] and the CEB-FIP Model Code 2010

[17]. The Bazant expression, shown as Equation 2, is a function of compressive strength, type and maximum size of the aggregate and water-to-cement ratio, while the JSCE-07 relationship, shown as Equation 3, is a function of compressive strength and maximum aggregate size, and the CEB-FIP Model Code 2010 relationship, shown as Equation 4, is only a function of compressive strength.

As shown in Table 4, the Bazant and CEB-FIP Code equation showed good agreement with the test data, with most of the test values falling within 10% of the predicted fracture energies. The JSCE-07 expression, on the other hand, noticeably underestimated the fracture energies between 12% and 34%.

$$G_F = 2.5\,\alpha_o \left(\frac{fc'}{0.051}\right)^{0.46} \left(1+\frac{d_a}{11.27}\right)^{0.22} \left(\frac{w}{c}\right)^{-0.30} \quad \text{(N/m)} \qquad (2)$$

$$G_F = 10 d_{\max}^{0.33} f_{ck}^{0.33} \quad \text{(N/m)} \qquad (3)$$

$$G_F = 73 f_{cm}^{0.18} \quad \text{(N/m)} \qquad (4)$$

where

α_0 = 1 for rounded aggregate and 1.44 for crushed or angular aggregate.

d_a = maximum aggregate size (mm);

d_{max} = maximum aggregate size (mm);

f_c’ = specified compressive strength of concrete (MPa);

f_{ck} = characteristic compressive cylinder strength of concrete (MPa);

f_{cm} = mean compressive strength of concrete (MPa);

w/c = water to cement ratio.

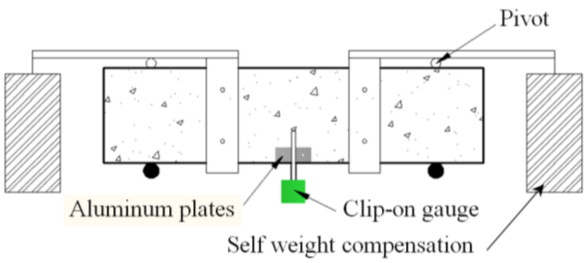

a) Fracture specimen

b) Test set up

Fig. 1 Fracture energy specimen and test set up

TABLE 3 Normalize Fracture Energy Based on Different Equations

Mix		CC	RCA-30	RCA-50	RCA-70	RCA-100
f'_c (MPa)		37.2	44.5	45.5	35.2	34.1
w/c		0.45	0.45	0.47	0.47	0.5
G_F (N/m)		148.7	151.1	138.1	126.2	98.9
		146.4	151.2	148.1	124.3	105.6
		138.7	138.3	146.2	121.2	106.2
		144.1	154.8	141.8	120.3	112.9
Bazant Eq.	G^{N*}_F (N/m)	22.2	20.8	19.0	19.6	15.8
		21.8	20.8	20.4	19.3	16.9
		20.7	19.0	20.1	18.8	17.0
		21.5	21.3	19.5	18.6	18.1
JSCE Eq.	G^{N*}_F (N/m)	45.1	43.2	39.2	39.0	30.9
		44.4	43.2	42.0	38.4	32.9
		42.1	39.5	41.5	37.4	33.1
		43.7	44.3	40.2	37.2	35.2
CEB-FIP Eq.	G^{N*}_F (N/m)	77.5	76.3	69.5	66.5	52.4
		76.3	76.4	74.5	65.5	55.9
		72.4	69.9	73.5	63.9	56.3
		75.1	78.2	71.3	63.4	59.8

*: Normalized

TABLE 4 Fracture Energy (G_F)

Mix	CC	RCA-30	RCA-50	RCA-70	RCA-100
f^*c	37.2	44.5	45.5	35.2	34.1
G^{**}_F	148.7	151.1	138.1	126.2	98.9
	146.4	151.2	148.1	124.3	105.6
	138.7	138.3	146.2	121.2	106.2
	144.1	154.8	141.8	120.3	112.9
$G_{F(AVE.)}$	144.5	148.9	143.5	123.0	105.9
$G_{F(Bazant.)}$	122.7	133.3	132.9	118.1	114.3
$G_{F(JSCE)}$	95.4	101.2	102.0	93.7	92.7
$G_{F(CEB\text{-}FIP)}$	140.0	144.6	145.1	138.6	137.8
$\left(\frac{G_{F(Bazant)}}{G_{F(test)}}\right)$	0.85	0.90	0.93	0.96	1.08
$\left(\frac{G_{F(JSCE)}}{G_{F(test)}}\right)$	0.66	0.68	0.71	0.76	0.88
$\left(\frac{G_{F(CEB\text{-}FIP)}}{G_{F(test)}}\right)$	0.97	0.97	1.01	1.13	1.30

*: MPa
**: N/m

Figure 2 is a plot of fracture energy as a function of compressive strength. Included in the plot are the results of the current study as well as the inventory of fracture energy test data available in the literature [15]. Given the significant scatter of the database of fracture energy test results, it is somewhat difficult to draw definitive conclusions on the current test values. Nonetheless, visually, Figure 2 seems to indicate that all of the mixes test results fall within the upper portion of the data and follow the same general trend of increasing fracture energy as a function of compressive strength. More importantly, all of the mixes fracture energies from the current study are very consistent with each other when accounting for compressive strength, offering a valuable comparison among the concrete types. Furthermore, statistical analysis of the data (using regression analysis to draw the best fit and 95% confidence intervals) indicates that all five mixes test results fall within and slightly above a 95% confidence interval of a nonlinear regression curve fit of the database. This result indicates that the test values are also consistent with the wealth of fracture energy test data available in the literature.

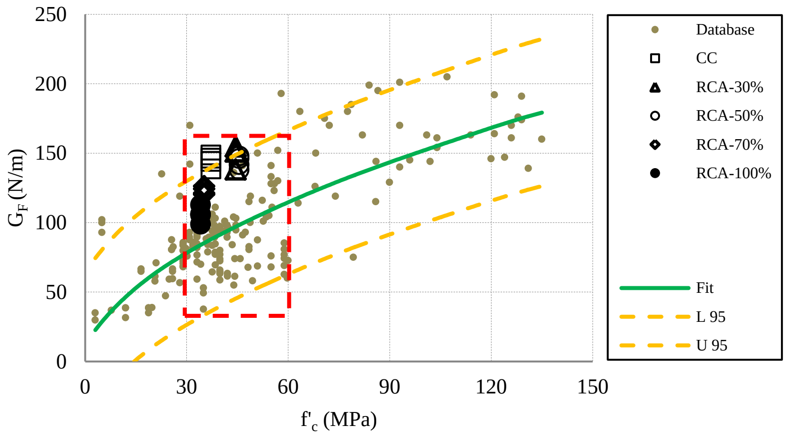

a)

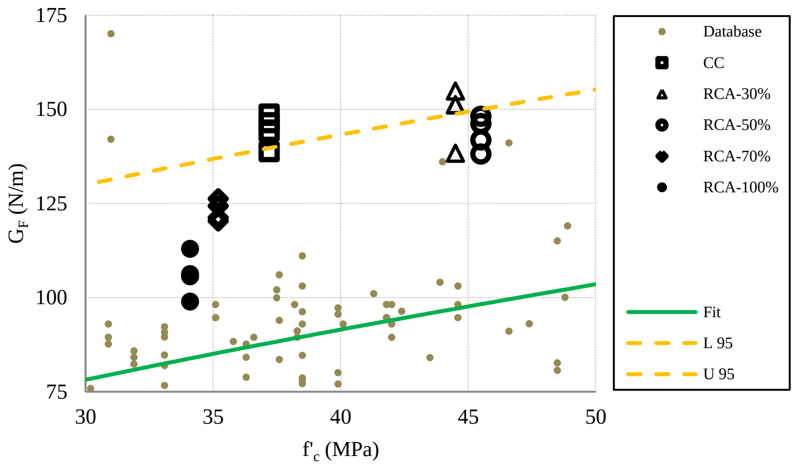

b)

Fig. 2 Fracture energy vs. compressive strength; results from literature [15] and test results of this study

V. STATISTICAL DATA ANALYSIS

To compare the fracture energy test results of the five mixes, the results must be adjusted to reflect the different compressive strengths and water-to-cement ratios. Fracture energy is a function of the compressive strength with powers of 0.46, 0.33, and 0.18 based on the Bazant et al., the JSCE-07, and the CEB-FIP Model Code 2010, respectively and also water cement ratio only in the Bazant equation. Therefore, to normalize the data for comparison, the fracture energies were divided by the aforementioned powers of the compressive strengths and also water cement ratio for the Bazant equation. As mentioned above, Table 3 presents the normalized fracture energies for different mixes based on three aforementioned equations.

Statistical tests (both parametric and nonparametric) were used to evaluate whether there is any statistically significant difference between the fracture energy test results for all mixes.

B. Parametric Test

The paired t-test is a statistical technique used to compare two population means. This test assumes that the differences between pairs are normally distributed. If this assumption is violated, the paired t-test may not be the most powerful test. The hypotheses for the paired t-tests for fracture energies are as follows:

H_{o1}: The mean of the normalized fracture energy of the RCA-30% mix is lower than the CC mix [$G_{F\ (RCA\ -30\%)} < G_{F\ (CC)}$].

H_{o2}: The mean of the normalized fracture energy of the RCA -50% mix is lower than the CC mix [$G_{F\ (RCA\ -50\%)} < G_{F\ (CC)}$].

H_{o3}: The mean of the normalized fracture energy of the RCA -70% mix is lower than the CC mix [$G_{F\ (RCA\ -70\%)} < G_{F\ (CC)}$].

H_{o4}: The mean of the normalized fracture energy of the RCA -100% mix is lower than the CC mix [$G_{F\ (RCA\ -100\%)} < G_{F\ (CC)}$].

H_{o5}: The mean of the normalized fracture energy of the RCA -50% mix is lower than the RCA -30% mix [$G_{F\ (RCA\ -50\%)} < G_{F\ (RCA\ -30\%)}$].

H_{o6}: The mean of the normalized fracture energy of the RCA -70% mix is lower than the RCA -30% mix [$G_{F\ (RCA\ -70\%)} < G_{F\ (RCA\ -30\%)}$].

H_{o7}: The mean of the normalized fracture energy of the RCA -100% mix is lower than the RCA -30% mix [$G_{F\ (RCA\ -100\%)} < G_{F\ (RCA\ -30\%)}$].

H_{o8}: The mean of the normalized fracture energy of the RCA -70% mix is lower than the FA-50% mix [$G_{F\ (RCA\ -70\%)} < G_{F\ (RCA\ -50\%)}$].

H_{o9}: The mean of the normalized fracture energy of the RCA -100% mix is lower than the RCA -50% mix [$G_{F\ (RCA\ -100\%)} < G_{F\ (RCA\ -50\%)}$].

H_{o10}: The mean of the normalized fracture energy of the RCA -100% mix is lower than the RCA -70% mix [$G_{F\ (RCA\ -100\%)} < G_{F\ (RCA\ -70\%)}$].

H_a: Not H_o

The statistical computer program SAS 9.2 was employed to perform these statistical tests. Both Kolmogorov-Smirnov (K-S) and Anderson-Darling (A-D) tests showed the data – the differences between the fracture energies of the mixes – follow a normal distribution. Therefore, the paired t-test could be performed. Table 5-a summarizes the result of the paired t-tests (p-values at the 0.05 significance level). All p-values were greater than 0.05, which means that the null hypotheses at the 0.05 significance level are confirmed. In other words, the higher RCA replacement levels, the lower fracture energies.

C. Nonparametric Test

Unlike the parametric tests, nonparametric tests are referred to as distribution-free tests. These tests have the advantage of requiring no assumption of normality, and they usually compare medians rather than means. The Wilcoxon signed-rank test is usually identified as a nonparametric alternative to the paired t-test. The hypothesis for this test is the same as that for the paired t-test except that median is used instead of mean value. The Wilcoxon signed-rank test assumes that the distribution of the difference of pairs is symmetrical. This assumption can be checked; if the distribution is normal, it is also symmetrical. As mentioned earlier, the data follow normal distribution and the Wilcoxon signed-rank test can be used. Table 5-b summarizes the results of the Wilcoxon signed-rank test (p-values at the 0.05 significance level). All p-values were greater than 0.05 that means the null hypothesis at the 0.05 significance level are confirmed.

Results of the statistical data analyses showed that the mix with higher percentage of RCA replacement level has lower fracture energy.

The lower fracture energy of RCA mix can be attributed to two interfacial zones (ITZ) of RCA: one between virgin aggregate and residual mortar and the other between residual mortar and fresh mortar, however for CC, there is only one ITZ between virgin aggregate and fresh mortar. As mentioned above, the existence of two ITZ for RCA mixes makes a weaker link for RCA compared with CC mix. This hypothesis was confirmed by comparing the RCA mixes with higher percentage of recycled aggregate replacement, and the weaker links mean lower fracture energies.

However, due to the limited nature of the data set regarding mix designs, aggregate type and content, etc., the authors recommend further tests to increase the database of test results and confirm this hypothesis.

VI. FINDINGS AND CONCLUSIONS

The purpose of this study was to compare fracture energy of mixes with different percentages of RCA as a coarse aggregate replacement. Based on the results of this study, the following findings and conclusions are presented:

- Statistical test results show that the fracture energy decreases with the increasing RCA replacement level.
- The JSCE-07 provision underestimates the fracture energy for all specimens.
- The CEB-FIP Model Code 2010 and Bazant equations have a good agreement with the test results of this study.
- The normalized fracture energies of all mixes fall within and slightly above the 95% confidence interval of a nonlinear regression curve fit of the database of previous fracture energy tests of CC specimens.

TABLE 5 COMPARISON OF FRACTURE ENERGY (GF) FOR DIFFERENT MIXES

a) P-value for parametric test (paired t-test)

Equation	CC > RCA 30	CC > RCA 50	CC > RCA 70	CC > RCA 100
Bazant	0.979	0.977	0.999	0.997
JSCE	0.921	0.965	1.000	0.998
CEB-FIP	0.551	0.899	1.000	0.998

Equation	RCA30 > RCA 50	RCA30 > RCA 70	RCA30 > RCA 100
Bazant	.802	0.965	0.995
JSCE	0.855	0.989	0.998
CEB-FIP	0.840	0.995	0.998

Equation	RCA50 > RCA 70	RCA50 > RCA 100
Bazant	0.901	0.995
JSCE	0.975	0.998
CEB-FIP	0.992	0.999

Equation	RCA70 > RCA 100
Bazant	0.976
JSCE	0.985
CEB-FIP	0.986

b) P-value for Non-parametric test (Wilcoxon signed rank test)

Equation	CC > RCA 30	CC > RCA 50	CC > RCA 70	CC > RCA 100
Bazant	0.978	0.978	0.978	0.978
JSCE	0.95	0.978	0.978	0.978
CEB-FIP	0.572	0.95	0.978	0.978

Equation	RCA30 > RCA 50	RCA30 > RCA 70	RCA30 > RCA 100
Bazant	0.899	0.978	0.978
JSCE	0.895	0.978	0.978
CEB-FIP	0.897	0.978	0.978

Equation	RCA50 > RCA 70	RCA50 > RCA 100
Bazant	0.95	0.978
JSCE	0.978	0.978
CEB-FIP	0.978	0.978

Equation	RCA70 > RCA 100
Bazant	0.978
JSCE	0.985
CEB-FIP	0.978

ACKNOWLEDGMENT

The authors gratefully acknowledge the financial support provided by the Missouri Department of Transportation (MoDOT) and the National University Transportation Center at Missouri University of Science and Technology. The authors would also like to thank the support staff in the Department of Civil, Architectural and Environmental Engineering and Center for Infrastructure Engineering Studies at Missouri S&T for their efforts. The conclusions and opinions expressed in this paper are those of the authors and do not necessarily reflect the official views or policies of the funding institutions.

REFERENCES

[1] Malhotra, V.M. (1986). “Superplasticized Fly Ash Concrete for Structural Applications,” Concrete International, V.8, pp. 28- 31.

[2] Arezoumandi, M., Volz, J. S., Ortega, C. A., & Myers, J. J. (2013). “Effect of Total Cementitious Content on Shear Strength of High-Volume Fly Ash Concrete Beams.” Materials & Design, 46, 301-309.

[3] Arezoumandi, M., Volz, J. S., & Myers, J. J. (2012). “Shear Behavior of High-Volume Fly Ash Concrete versus Conventional Concrete. “ Journal of Materials in Civil Engineering. doi:10.1061/(ASCE)MT.1943-5533.0000700.

[4] Arezoumandi, M., Wolfe, M. H., & Volz, J. S. (2013). “A comparative study of the bond strength of reinforcing steel in high-volume fly ash concrete and conventional concrete.” Construction and Building Materials, 40, 919-924.

[5] Arezoumandi, M., Smith, A., Volz, J. S., Khayat, K. H. (2013). “An Experimental Study on Shear Strength of Reinforced Concrete Beams with 100% Recycled Concrete Aggregate” Construction and Building Materials, DOI: 10.1016/j.conbuildmat.2013.12.019.

[6] Bordelon, A., Cervantes, V., & Roesler, J. R. (2009). Fracture properties of concrete containing recycled concrete aggregates. Magazine of Concrete Research, 61(9), 665-670.

[7] Casuccio, M., Torrijos, M. C., Giaccio, G., & Zerbino, R. (2008). Failure mechanism of recycled aggregate concrete. Construction and Building Materials, 22(7), 1500-1506.

[8] World Business Council for Sustainable Development (WBCSD) Report (2012). “Recycling concrete” http://www.wbcsdcement.org/index.php/key-issues/sustainability-with-concrete/54, Accessed date: August 2013.

[9] Bažant, Z. P., and Yu, Q., (2005) "Design against Size Effect on Shear Strength of Reinforced Concrete Beams without Stirrups," Journal of Structural Engineering, ASCE, V. 131, No. 12, pp. 1877-1885.

[10] Gastebled, O. J., and May, I. M., (2001) "Fracture Mechanics Model Applied to Shear Failure of Reinforced Concrete Beams without Stirrups," ACI Structural Journal, V. 98, No. 2, pp. 184-190.

[11] Xu, S., Zhang, X., and Reinhardt, H.s W., (2012) "Shear Capacity Prediction of Reinforced Concrete Beams without Stirrups Using Fracture Mechanics Approach," ACI Structural Journal, V. 109, No. 5, pp. 705-714.

[12] ACI Committee 408. (2003). "Bond and Development of Straight Reinforcing Bars in Tension" (ACI 408R-03). Farmington Hills, MI: American Concrete Institute.

[13] Hillerborg, A. (1985) "The Theoretical Basis of a Method to Determine the Fracture Energy GF of Concrete," Materials and Structures, V. 18, No. 106, pp. 291-296.

[14] RILEM, 1985, TC 50-FMC, Fracture Mechanics of Concrete, "Determination of the Fracture Energy of Mortar and Concrete by Means of Three-Point Bend Tests on Notched Beams," RILEM Recommendation, Materials and Structures, V. 18, No. 16, pp. 287-290.

[15] Bazant, Z.P., and Becq-Giraudon, E., (2002), Statistical prediction of fracture parameters of concrete and implications for choice of testing standards. Cement and Concrete Research Journal, Vol. 32, No. 4, pp. 529-556.

[16] Japan Society of Civil Engineers (2007). "Standard Specification for Concrete Structure" JSCE No. 15, Tokyo, pp. 154-159.

[17] CEB-FIP Model Code 2010-fib (2012), Vol. 1, p.120.

Mahdi Arezoumandi is a postdoctoral research fellow in the School of Civil Engineering and Environmental Science at the University of Oklahoma, US. He received his BS and MS from Amirkabir University, Tehran, Iran and PhD from Missouri University of Science and Technology, US. He is a member of ACI Committee 408 (Development and Splicing of Deformed Bars) and ACI Committee 445 (Shear and Torsion). His research interest is structural behavior of sustainable concrete.

Jonathan Drury is a PhD student in the School of Civil Engineering and Environmental Science at the University of Oklahoma. He received his BS and MS from Missouri University of Science and Technology, US.

Jeffery S. Volz is an associate professor in the School of Civil Engineering and Environmental Science at the University of Oklahoma. He received his BAE, MS, and PhD from The Pennsylvania State University, US. He is a member of Joint ACI-ASCE Committee 423 (Prestressed Concrete) and ACI Committees 123 (Research and Current Developments), 130 (Sustainability of Concrete), 215 (Fatigue of Concrete), and 222 (Corrosion of Metals in Concrete). His research interests include durability, repair, and material improvements of cementitious systems.